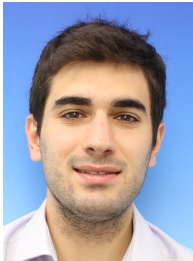


Large Scale Tri-Generation Energy Storage System for Heat, Cold and Electricity based on Transcritical CO₂ Cycles

Luis Sanz Garcia*
Development Engineer
MAN Energy Solutions Schweiz AG
Zurich, Switzerland

Emmanuel Jacquemoud
Technical Project Manager
MAN Energy Solutions Schweiz AG
Zurich, Switzerland

Philipp Jenny
Head of R&D Centrifugal Compressor Engineering
MAN Energy Solutions Schweiz AG
Zurich, Switzerland



Luis Sanz Garcia graduated from École Polytechnique Fédérale de Lausanne (EPFL) with a Master of Science in Mechanical Engineering. Currently working at MAN Energy Solutions Schweiz AG, where his main tasks consists on development of thermodynamic and costing models of the different components of the Electro Thermal Energy Storage (ETES) system in order to better understand and optimize the system's thermo-economic performance.



Emmanuel Jacquemoud graduated from the ETH Zürich with a Master of Science in Mechanical Engineering. Currently working at MAN Energy Solutions Schweiz AG, with previous experience in the thermodynamic design of turbomachines, rotordynamics and troubleshooting, he is now responsible for the technical development of the ETES system.



Philipp Jenny graduated with a Dual Master of Science in Mechanical Engineering from EPFL Lausanne and in Aerospace Engineering from École Nationale Supérieure de l'Aéronautique et de l'Espace (ISAE-SUPAERO). He obtained his PhD in Mechanical Engineering from ETH Zurich. Currently working at MAN Energy Solutions Schweiz AG, where he has a R & D responsibility for Centrifugal Compressor Solutions.

ABSTRACT

Technical, political and social challenges to meet the ambitious decarbonisation goals, combined with increased fluctuating renewable energy (REN) sources, require the development of innovative large-scale energy storage systems. Heating and cooling applications contribute to over 51% of the worldwide total energy consumption [1] and raise the question how to integrate energy systems in the most economic and efficient way, i.e. as close as possible to the final

*luis.sanz-garcia@man-es.com

energy demand form for future sustainable cities.

A moderate temperature (0-150°C) tri-generation electro-thermal energy storage system (designated 3-TES) is introduced to fulfill the final consumption side boundary conditions, (a) heating or/and cooling demand, (b) electricity re-transformation, or (c) the three energy flux forms combined together. The system comprises efficient and scalable turbomachinery to compress the process medium (CO₂) to supercritical conditions followed by an expansion to subcritical thermodynamic state and intermediate tailor-made heat exchangers to optimize energy transfer conditions. The process is operated in both Heat Pump (i.e. charging) and Heat Engine (i.e. discharging) modes. Various applications use cases with varying energy demand profiles, scaling configurations and operating boundary conditions show that 3-TES is a very versatile and efficient energy storage system that may contribute future decarbonization pathways. This is shown in this paper by the system architecture and model description first, then the impact of the major boundary conditions on the system performance and economics and finally the operational flexibility over typical use cases.

NOMENCLATURE

Acronyms

3-TES	Trigeneration Electro-Thermal Energy Storage
AA-CAES	Advanced Adiabatic Compressed Air Energy Storage
CAPEX	Capital expenditure [€]
D-CAES	Diabatic Compressed Air Energy Storage
ETES	Electro-Thermal Energy Storage
HE	Heat engine
HP	Heat pump
LAES	Liquid Air Energy Storage

Greek Symbols

η	Efficiency [%]
γ	Stored energy share [%]
ϕ	Ratio between export energy and charging electricity costs [-]
Π	Pressure ratio [-]
θ	Stored thermal energy [MWh _{th}]
ξ	Thermal export efficiency [%]

Other Symbols

ΔT	Temperature difference [K]
C	Cost of energy [€/MWh]
COP	Coefficient of performance [-]

E	Electric energy [MWh _{el}]
P_{cy}	Profit per cycle [€]
Pen	Optimization penalty [-]
Q	Thermal energy [MWh _{th}]
T	Temperature [°C]
t	Cycle time [h]

Superscripts

bal	Balanced
cy	Thermodynamic cycle
el	Electric export
ex	Total export
pp	Pinch point
ret	Return
sup	Supply
th	Thermal export
tot	Total: sum of electric and thermal

Subscripts

ch	Charging cycle
$cold$	Cold export cycle
dch	Discharging cycle
HE	Heat engine
hot	Hot export cycle
RT	Round-trip

INTRODUCTION

Large-scale energy storage solutions for electricity, e.g. Pumped Hydro or Compressed Air Energy Storage (CAES), exist for decades already and are designed to balance the electricity grid and to cope with renewable energy sources integration into the energy mix. However, the geological dependency limitations of these solutions promote the need for location independent large scale energy storage solutions. The ABB corporate research center developed the Electro-Thermal Energy Storage (ETES) as a site independent electricity-only storage system [2] using a CO₂ thermodynamic cycle. During the charging cycle the system operates in a heat pump (HP) mode and produces hot and cold thermal energy that is stored in the form of hot water and ice. In the discharging cycle the stored thermal energy provides the hot and cold energy source for the heat engine (HE) cycle that generates electricity back to the grid. Figure 1

shows the ABB designed ETES charging and discharging thermodynamic cycles.

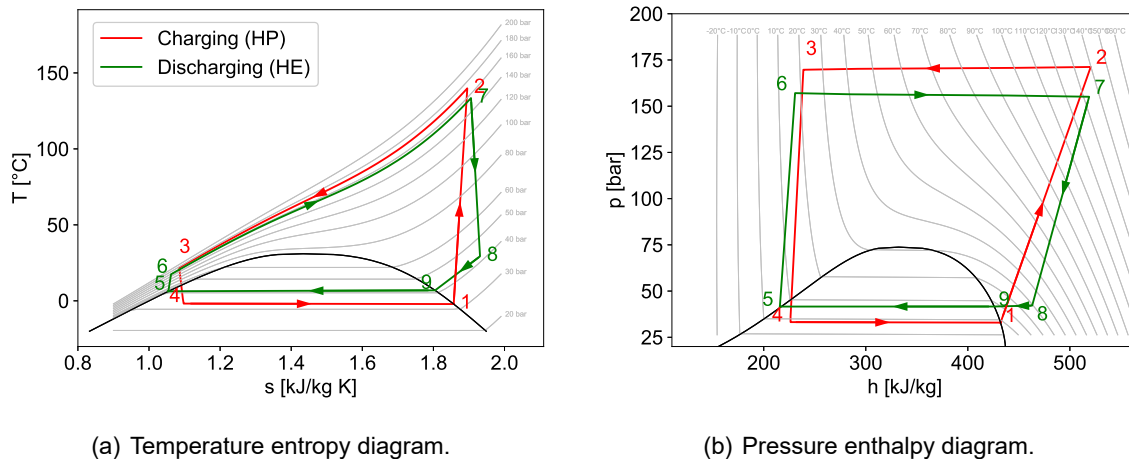


Figure 1: ETES charging and discharging thermodynamic cycles.

The ABB ETES research and development [3], [4], [5], [6] focuses on seeking for the highest possible round-trip efficiency (see Equation 1) as the key electricity-to-electricity energy storage system performance indicator. This parameter quantifies the ratio between the discharged electrical energy E_{dch} and the required electricity E_{ch}^{el} used to charge the system. MAN Energy Solutions Schweiz AG has developed the so-called tri-generation Electro-Thermal Energy Storage system (3-TES) based on the original ABB designed system but extended it to a **heat and cold storage system that also provides electricity**. A 3-TES system operator has therefore the flexibility to use the stored energy amount for heat and cold exportation and re-electrification. Since 81% of the European heating and cooling energy demand is needed for temperatures lower than 200°C [7], the 3-TES moderate temperature level (see Table 1) offers different options to balance most of the industrial electrical and thermal energy demands and to integrate renewable energy electrical sources in the energy mix so to support the de-carbonization goals.

Thermal Storage	Medium	Temperature range	Type	Setup
Hot	Water	15-150 °C	Sensible	Multi-tank reservoirs
Cold	Water / Ice	0 °C	Latent	Ice on coils

Table 1: 3-TES hot and cold thermal storages conditions.

In terms of sizing, the dimension of the system is limited by the existing turbomachinery, allowing to conceive systems in the 1-50 MW_{el} power range. Typical cycle times t_{tot} (charging and discharging) of the 3-TES system are defined by the fluctuation in the electricity prices as well as the capital expenditure of the thermal storages. Therefore, although cycles times below 8 hours are still feasible, the cycle is expected to obtain optimum trade-off between CAPEX and OPEX when operating from one to two cycles per day (i.e. cycle times between 12 to 24 hours).

ARCHITECTURE AND WORKING PRINCIPLE OF THE 3-TES SYSTEM

Figure 2 shows the 3-TES schematic representation that includes turbomachinery, heat exchangers and thermal storage. The main differences to the original ABB designed ETES configuration are the hot and cold energy export additional interfaces and an optimized turbomachinery arrangement for the charging and discharging cycles.

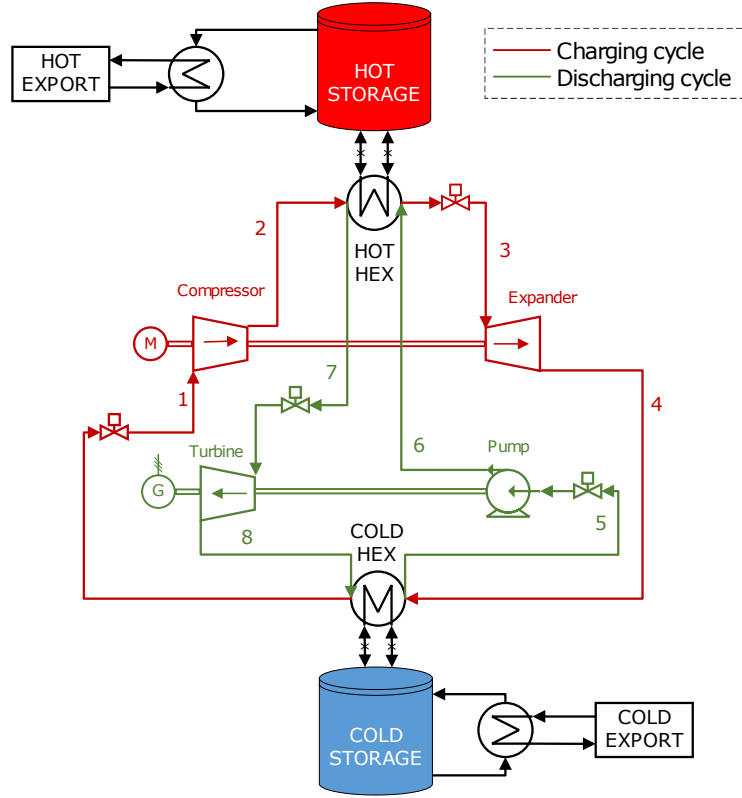


Figure 2: Schematic representation of the tri-generation (3-TES) system architecture.

The working principle, main thermodynamic parameters for the transcritical charging and discharging cycles (see Figure 1), and process medium (CO_2) is practically the same as the original ETES design. However the novel 3-TES functionalities require revised and extended system performance indicators. In addition to the electrical round-trip-efficiency η_{RT} (Equation 1), the thermal export coefficient of performance $COP_{hot,cold}^{ex}$ (Equation 2) measures the efficiency for which the system produces heat and cold energy $Q_{hot,cold}$ per electrical energy stored for the thermal exports purpose E_{ch}^{th} .

$$\eta_{RT} = \frac{E_{dch}}{E_{ch}^{el}} \quad (1) \quad COP_{hot,cold}^{ex} = \frac{Q_{hot,cold}}{E_{ch}^{th}} \quad (2)$$

Compared to other energy storage systems where only one energy form can be exported (thermal or electric), the 3-TES system operator has the flexibility to choose the stored electrical energy amount destined for heating and cooling (E_{ch}^{th}) or/and for re-electrification (E_{ch}^{el}). The **thermal share** (γ^{th}) and **electric share** (γ^{el}) define the stored electrical energy percentage for thermal export and re-electrification, respectively (see Equation 3).

$$E_{ch}^{tot} = E_{ch}^{th} + E_{ch}^{el} = E_{ch}^{tot} \cdot \gamma^{th} + E_{ch}^{tot} \cdot \gamma^{el} = E_{ch}^{tot} \cdot (\gamma^{th} + \gamma^{el}) \Rightarrow \gamma^{th} + \gamma^{el} = 1 \quad (3)$$

A thermal share of $\gamma^{th} = 100\%$ corresponds to a pure heat pump operation with only thermal export. A thermal share of $\gamma^{th} = 0\%$ corresponds to a only heat engine operation with re-electrification of all the thermal energy.

The stored thermal energy $\theta_{hot,cold}$ is equal to the electricity input multiplied by the HP cycle hot and cold coefficient of performance $COP_{hot,cold}^{cy}$ (see Equation 4). The stored thermal energy $\theta_{hot,cold}$ multiplied by the thermal and electric share determines how much stored thermal energy is available for each energy export form.

$$\theta_i^{tot} = E_{ch}^{tot} \cdot COP_i^{cy} = \theta_i^{th} + \theta_i^{el} \Rightarrow \begin{cases} \theta_i^{th} = \theta_i^{tot} \cdot \gamma^{th} \\ \theta_i^{el} = \theta_i^{tot} \cdot \gamma^{el} \end{cases} \quad i = hot, cold \quad (4)$$

Once the stored energy for thermal export and electricity generation is defined, **the 3-TES can be considered as two independent sub-systems:**

1. **Heat pump with storage tanks as buffer.** Based on Equation 2, Equation 5 presents this sub-system's efficiency in more detail. Thermal export efficiency $\xi_{hot,cold}$ represents the share of stored thermal heat that can be used to provide heat for given temperature levels on the consumer side. The amount of thermal energy which cannot be used $Q_{hot,cold}^{bal}$ must be balanced to restore thermal equilibrium in the system.

$$COP_i^{ex} = \frac{Q_i}{E_{ch}^{th}} = \frac{\theta_i^{th} \cdot \xi_i}{E_{ch}^{th}} = COP_i^{cy} \cdot \xi_i \quad i = hot, cold \quad (5)$$

2. **Electricity-to-electricity storage system** (e.g. Pumped Hydro, CAES, LAES or original ETES). Equation 6 presents this sub-system round-trip efficiency and the value is directly proportional to the charging and discharging cycles key performance indicators.

$$\eta_{RT} = \frac{E_{dch}^{el}}{E_{ch}^{el}} = \frac{\theta_{hot}^{el} \cdot \eta_{HE}}{E_{ch}^{el}} = COP_{hot}^{cy} \cdot \eta_{HE} \quad (6)$$

Equation 7 shows the total energy comprises the above subsystems in three energy forms, (a) hot, (b) cold, and (c) electricity, that must obey together the conservation of energy law.

$$E_{ch}^{tot} \cdot \begin{cases} \gamma^{th} \cdot COP_{hot}^{ex} & = Q_{hot} \\ \gamma^{th} \cdot COP_{cold}^{ex} & = Q_{cold} \\ \gamma^{el} \cdot COP_{hot}^{cy} \cdot \eta_{HE} & = E_{dch} \end{cases} \quad (7)$$

Figure 3 presents in a graphical illustration by means of a Sankey diagram a typical 3-TES cycle energy balance.

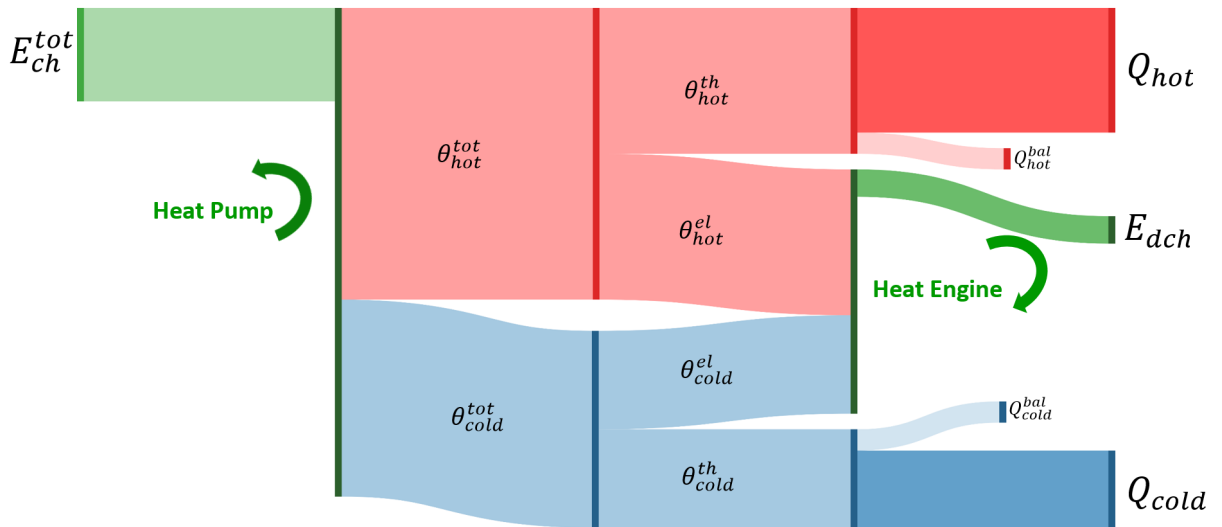


Figure 3: 3-TES energy balance with $\gamma^{th} = 50\%$.

MODEL DESCRIPTION

In order to find the optimum 3-TES configuration for given plant boundary conditions, a steady-state model has been developed to predict accurately the system performance and key component sizing and costing. The model has been developed in Python and uses NIST REFPROP [8] to calculate thermodynamic and transport properties of the process fluids CO₂ and water. The final plant design is determined using performance and costing models by sequentially solving energy balances component after component. Each key component is sized in collaboration with equipment suppliers and takes into account the respective manufacturer design rules, limitations and performances. Most components are modeled based on zero-dimensional models, the assumed efficiencies of which are shown in Table 2. Additionally, the heat exchanger modeling applies more refined thermodynamic models so to reach an acceptable level of prediction accuracy [6]. The overall model includes additional costs related to the engineering, civil, and procurement work so to reach finally a realistic total plant overall costing.

Component	Isentropic efficiency	Electrical efficiency
Compressor	80%	-
Expander	80%	-
Power turbine	88%	-
CO ₂ pump	80%	-
Auxiliary pumps	85%	-
Electric motors	-	95%
Generator	-	98%

Table 2: Assumed 3-TES main components efficiencies.

3-TES design feasibility is guaranteed when the optimal system intensive and extensive design parameters x bounded by upper and lower bounds (u_b and l_b respectively) are found by objective function $f(x)$ minimization. By implementation of penalties $Pen_i(x)$ in the objective function, the optimizer is guided towards solutions without component limitation violation and thus guaranteeing the feasibility of the system. A more detailed description of the optimization parameters and model is presented in [6].

Equation 8 shows the optimization problem formulation that is solved by the open-source solver OpenDino. The definition of the objective function $f(x)$ will depend on the available boundary conditions information. If prices and demands of the three forms of energy are known, the objective function is considered equal to the profit derived from the operation of the system (see Equation 10), which will include a negative sign in order to maximize its value. If fewer information is available, a weighted objective function with the key performance indicators of Equation 1 and Equation 2 is considered.

$$\begin{aligned}
 & \underset{x}{\text{minimize}} && f(x) + \sum_{i=1} Pen_i(x) \\
 & \text{subject to} && l_b \leq x \leq u_b, \\
 & && x \in \mathbb{R}
 \end{aligned} \tag{8}$$

IMPACT OF THERMAL BOUNDARY CONDITIONS ON SYSTEM'S PERFORMANCE

The heat pump COP is determined mainly by heat sink and source temperatures. For the 3-TES case (see Figure 2), the sink side is determined by the hot storage tank temperatures with

CO₂ at supercritical conditions. On the cold side, the brine (intermediate loop) temperature required to generate ice (below 0°C) determines the subcritical CO₂ evaporation temperature. The importance of pinch point ΔT_{pp} in all the heat exchangers as well as turbomachinery efficiencies are the main parameters impacting exergy losses of the system. For the 3-TES system with thermal export, additional exergy losses are expected as a result of the intermediate loop between customer and the CO₂ process loop, since heat is firstly transferred to the storage tanks and finally to the consumer via intermediate heat exchangers.

Unlike conventional heat pumps where the expansion process is performed via a throttling valve, in the 3-TES system an expander stage (3 → 4 in Figure 1) is used, that reduces the charging cycle exergy losses [9] and contributes to the COP optimization of the heat pump cycle. Besides, the temperature of the hot storage coldest water tank has to match well with the temperature seen on the CO₂ loop side at the expander inlet. As the temperature of the tanks may be influenced by the thermal export conditions, this is an additional constraint to be taken into account in the system design.

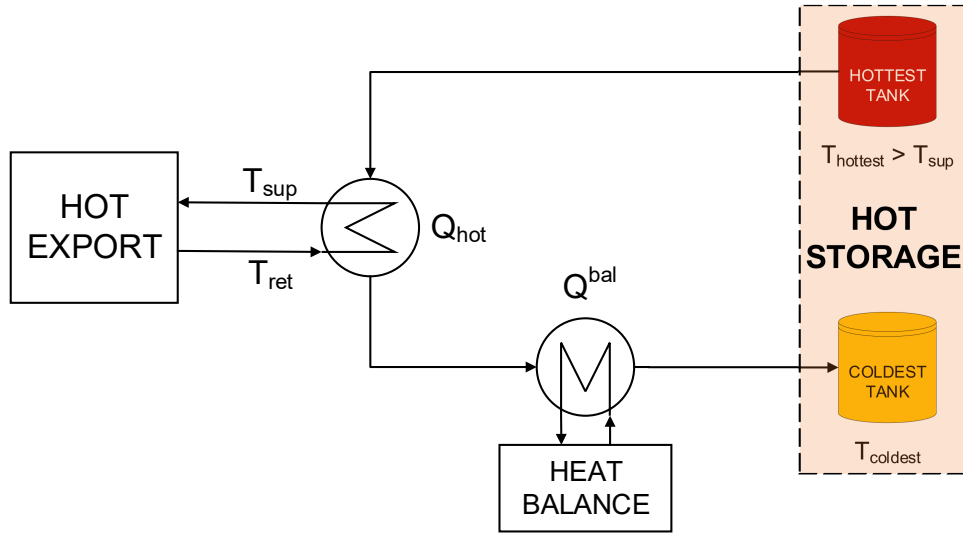


Figure 4: Schematic representation of the hot export interface.

For electricity generation this constraint does not represent a real issue since low temperatures at expander inlet are preferred to optimize η_{RT} , but it may become a concern when providing hot thermal export for certain boundary conditions. In worst case, the water from the hot thermal export loop should be cooled down to the level of the coldest hot storage temperature. In many applications the hot export return temperature T_{hot}^{ret} is higher than this temperature set point and therefore, a supplementary cooler must be introduced to balance the fluctuations in temperatures and bring the water back to the coldest tank temperature (see Figure 4). The energy required to cool down the water (Q^{bal}) can come from an ambient source (air, groundwater, sea, etc.) or from the generated cold energy available on site. The greater the temperature difference between the hottest temperature level and T_{hot}^{ret} , the larger the stored thermal energy share available for thermal export. Hence, the hottest and coldest tank temperatures are important parameters to maximize the hot thermal export performance.

The impact of higher consumer return temperature T_{hot}^{ret} is captured by the hot export efficiency ξ_{hot} , which represents the ratio between the heat transferred to the consumer circuit and produced by the charging cycle (see Equation 9). If part of the stored cold energy is used to cool down the water from the district heating loop the cold export efficiency ξ_{cold} is lower than 100% and hence, $Q_{hot}^{bal} = Q_{cold}^{bal} = Q^{bal}$.

$$\xi_{hot,cold} = \frac{Q_{hot,cold}}{Q_{hot,cold} + Q^{bal}} = \frac{Q_{hot,cold}}{\theta_{hot,cold}^{th}} \Rightarrow COP_{hot,cold}^{ex} = \xi_{hot,cold} \cdot COP_{hot,cold}^{cy} \quad (9)$$

As for any heat pump, the thermal export performance of the system depends above all on the boundary conditions set by the heat sink (hot export) and heat source (cold export). 3-TES cold energy is supplied by the cold brine at the evaporator exit or melting the stored ice if the charging cycle is not in operation. Since CO₂ evaporation temperature is determined by the water freezing temperature (0°C), the system's cold export performance (COP_{cold}^{ex}) can be considered independent of the cold temperature programs as long as the cold export supply temperature $T_{cold}^{sup} > 0^\circ\text{C}$ (large majority of applications). If temperatures lower than 0°C are requested, a different phase changing material is required, which combined with the increase in Π_{ch} causes higher investment costs and lower thermal export performance. The use of other phase changing materials could also be beneficial when higher cold export temperatures are required, allowing to evaporate at higher temperatures, reducing the temperature lift (i.e. charging pressure ratio Π_{ch}) to be carried out by the compressor and ultimately increase $COP_{hot,cold}^{cy}$ and therefore thermal export performance.

Considering a constant evaporation temperature, hot export requirements $T_{hot}^{ret,sup}$ are practically the only boundary conditions driving thermal export performance of the 3-TES system. As shown in Figure 5(a), the impact of Q^{bal} represents the biggest driver of 3-TES thermal export performance $COP_{hot,cold}^{ex}$. Cases with higher T_{hot}^{ret} result in higher Q^{bal} in order to reduce the water temperature down to the coldest tank temperature, meaning that a lower share of the stored thermal energy is available for thermal export (lower ξ_{hot} , see Equation 9). Moreover, COP_{hot}^{ex} degradation can be expected as a result of increasing T_{hot}^{ret} and T_{hot}^{sup} , requiring higher charging cycle pressure ratios Π_{ch} in order to meet the higher temperature requirements (see Figure 5(b)).

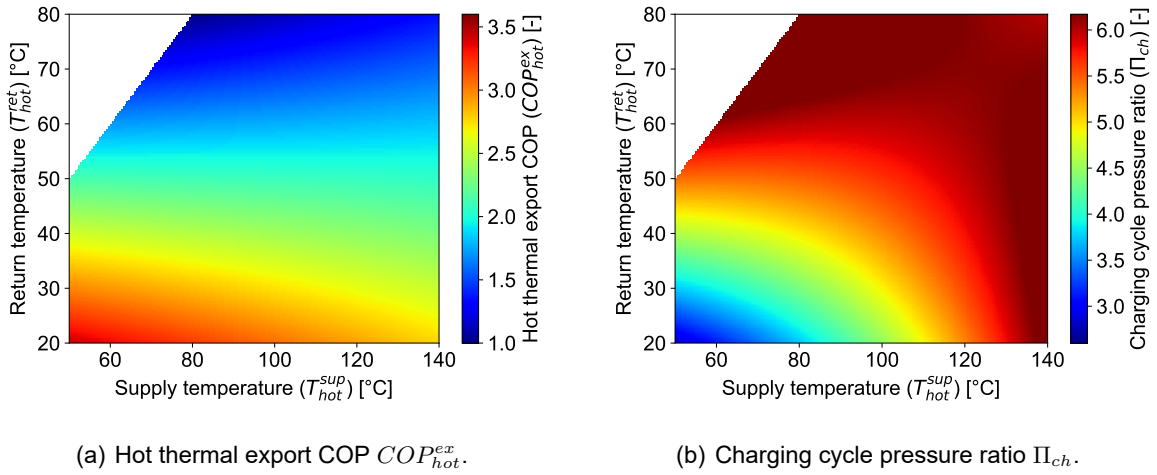


Figure 5: Impact of hot return and supply temperatures on COP_{hot}^{ex} and charging cycle pressure ratio Π_{ch} .

IMPACT OF ECONOMIC BOUNDARY CONDITIONS ON SYSTEM'S PERFORMANCE

The 3-TES system configuration design and optimization is linked to the three different forms of energy, their cost, and their fluctuation in demand and cost. For simplicity, heating (C_{hot}) and cooling (C_{cold}) costs are kept constant in this analysis. In contrast, electricity cost varies

throughout cycle time and requires two price definitions depending on the cycle: charging (C_{ch}^{el}) and discharging (C_{dch}^{el}). Equation 10 shows the total profit per cycle P_{cy} definition.

$$P_{cy}[\text{€}] = \left(E_{dch}^{el} \cdot C_{dch}^{el} + Q_{hot} \cdot C_{hot} + Q_{cold} \cdot C_{cold} \right) - E_{ch}^{tot} \cdot C_{ch}^{el} \quad (10)$$

The ratio between the export and charging electricity cost determines the optimal γ^{th} for the given boundary conditions. The impact of key performance indicators on profit can be derived from dividing P_{cy} per purchased energy amount $E_{ch}^{tot} \cdot C_{ch}^{el}$ as shown in Equation 11.

$$\begin{aligned} \frac{P_{cy}}{E_{ch}^{tot} \cdot C_{ch}^{el}} \left[\frac{\text{€}}{\text{€}_{ch}} \right] &= \frac{1}{E_{ch}^{tot} \cdot C_{ch}^{el}} \cdot (E_{dch}^{el} \cdot C_{dch}^{el} + Q_{hot} \cdot C_{hot} + Q_{cold} \cdot C_{cold}) - 1 \\ &= \left((1 - \gamma^{th}) \cdot \eta_{RT} \cdot \phi_{el} + \gamma^{th} \cdot (COP_{hot}^{ex} \cdot \phi_{hot} + COP_{cold}^{ex} \cdot \phi_{cold}) \right) - 1 \end{aligned} \quad (11)$$

Electricity export ($\gamma^{th} < 100\%$) should only be considered in situations where $\eta_{RT} > 1/\phi_{el}$. Equation 6 shows that η_{RT} depends on COP_{hot}^{cy} and η_{HE} , with both values dependent on the respective process cycle pressure ratio. Since the pressure ratio in the discharging cycle is lower than in the charging cycle, Π_{ch} , ΔT_{pp} , and turbomachinery efficiency determine the efficiencies of both cycles (COP_{hot}^{cy} and η_{HE} , respectively). Figure 6 shows that higher pressure ratio increases both the power required by the charging cycle and, from higher enthalpy difference in the power turbine, η_{HE} . The η_{HE} increase outweighs the COP_{hot}^{cy} decrease and therefore, electricity export configurations require highest possible Π_{ch} . The low pressure is limited by water freezing temperature (0°C) and compressor discharge pressure is limited by turbomachinery constraints and high pressurized tank costs; hence, since Π_{ch} is bound, so is η_{RT} .

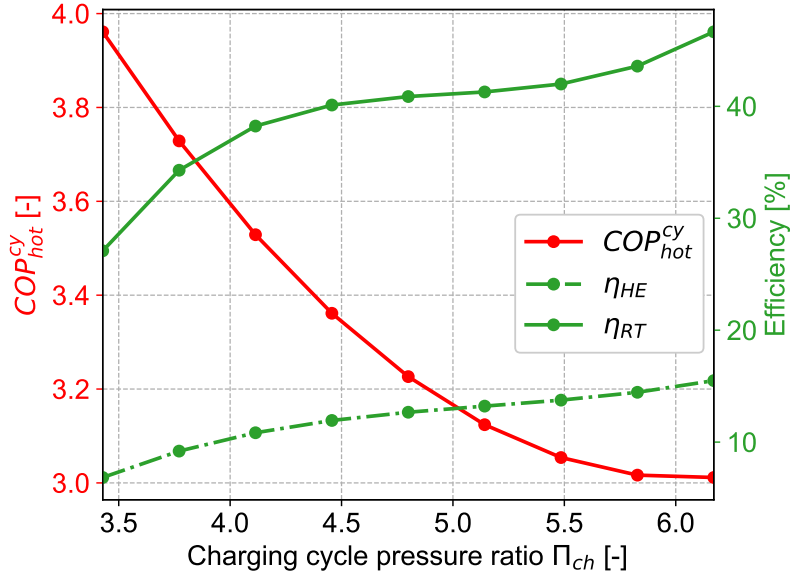


Figure 6: Impact of Π_{ch} on η_{RT} , η_{HE} and COP_{hot}^{cy} for a typical 3-TES example.

For thermal export ($\gamma^{th} > 0\%$), both hot and cold energies are exported and therefore require individual accounting. Equation 12 shows that both hot and cold export depend on COP_{hot}^{cy} and profit is dependent on system boundary conditions ($\phi_{hot,cold}$ and $\xi_{hot,cold}$).

$$\begin{aligned}
COP_{hot}^{ex} \cdot \phi_{hot} + COP_{cold}^{ex} \cdot \phi_{cold} &> 1 \\
COP_{hot}^{cy} \cdot \xi_{hot} \cdot \phi_{hot} + COP_{cold}^{cy} \cdot \xi_{cold} \cdot \phi_{cold} &> 1 \\
COP_{hot}^{cy} \cdot \xi_{hot} \cdot \phi_{hot} + (COP_{hot}^{cy} - 1) \cdot \xi_{cold} \cdot \phi_{cold} &> 1
\end{aligned} \tag{12}$$

$$COP_{hot}^{cy} > \frac{1 + \xi_{cold} \cdot \phi_{cold}}{\xi_{hot} \cdot \phi_{hot} + \xi_{cold} \cdot \phi_{cold}}$$

Thermal export COP_{hot}^{cy} maximization determines optimum Π_{ch} . The optimum cycle configuration selects Π_{ch} to maximize the total profit from both electricity and thermal export.

SYSTEM OPERATIONAL FLEXIBILITY

The 3-TES system flexibility to combine electrical and thermal energy export in a single system is well suited for multiple applications that vary from a heat pump ($\gamma^{th} = 100\%$) to a pure electrical utilization system ($\gamma^{th} = 0\%$). The optimal overall system configuration uses both electricity and thermal export functionalities ($0\% < \gamma^{th} < 100\%$). The optimum system size, configuration and γ^{th} depend on boundary conditions (energy demands, temperature programs, utility cost, etc.) specific to each application. Since boundary conditions are predicted to change during the plant's lifetime (>35 years), it is important that the system can adapt to varying conditions with a minimum additional investment.

To help better understand possible applications and advantages of the 3-TES system, the operation of a moderate size typical system (10 MW_{el} charging / 5 MW_{el} discharging) connected to the grid as well as to the hot and cold consumer network (district heating and cooling for instance) for three different days is presented in Figure 7.

The above example shows how the 3-TES thermal share shift (γ^{th}) is driven by utility cost fluctuations throughout the day (low and high tariffs), customer demands and capacity to operate at off-design conditions. The energy export, storage size utilization and cycle times vary depending on the selected approach to modify γ^{th} . The case presented in Figure 7 shows very different cycle operations depending on the energy demands and utility costs for a given and unchanged system configuration.

During Day 1, the lack of hot and cold demand results in the system operation as a pure electricity storage system ($\gamma^{th} = 0\%$), charging during periods of lower electricity prices and discharging whenever the price of electricity is higher, in this case with two charging and discharging cycles a day.

The advantage of the tri-generation energy storage system becomes evident for Day 2, where the presence of thermal demand from both hot and cold customers allows to increase significantly the revenue of the operator. Moreover, the existence of large peaks of wind renewable energy at night allows to charge the system to the highest possible storage level at negative prices and generate electricity during hours of low solar radiation and lack of wind later in the day, which result in high electricity prices (ref. to the peak revenue between 7-10 AM of Day 2). Compared to Day 1, the export of hot and cold thermal energy in Day 2 leads to mismatches in hot and cold storage levels throughout the cycle as a result of their different respective thermal load profiles. To bring the system back to energy balance may require additional auxiliary heat balancing equipment with higher system complexity and cost; however, the additional equipment benefits system usage and flexibility.

During Day 3, the smaller electricity price fluctuations make the system profitable only if

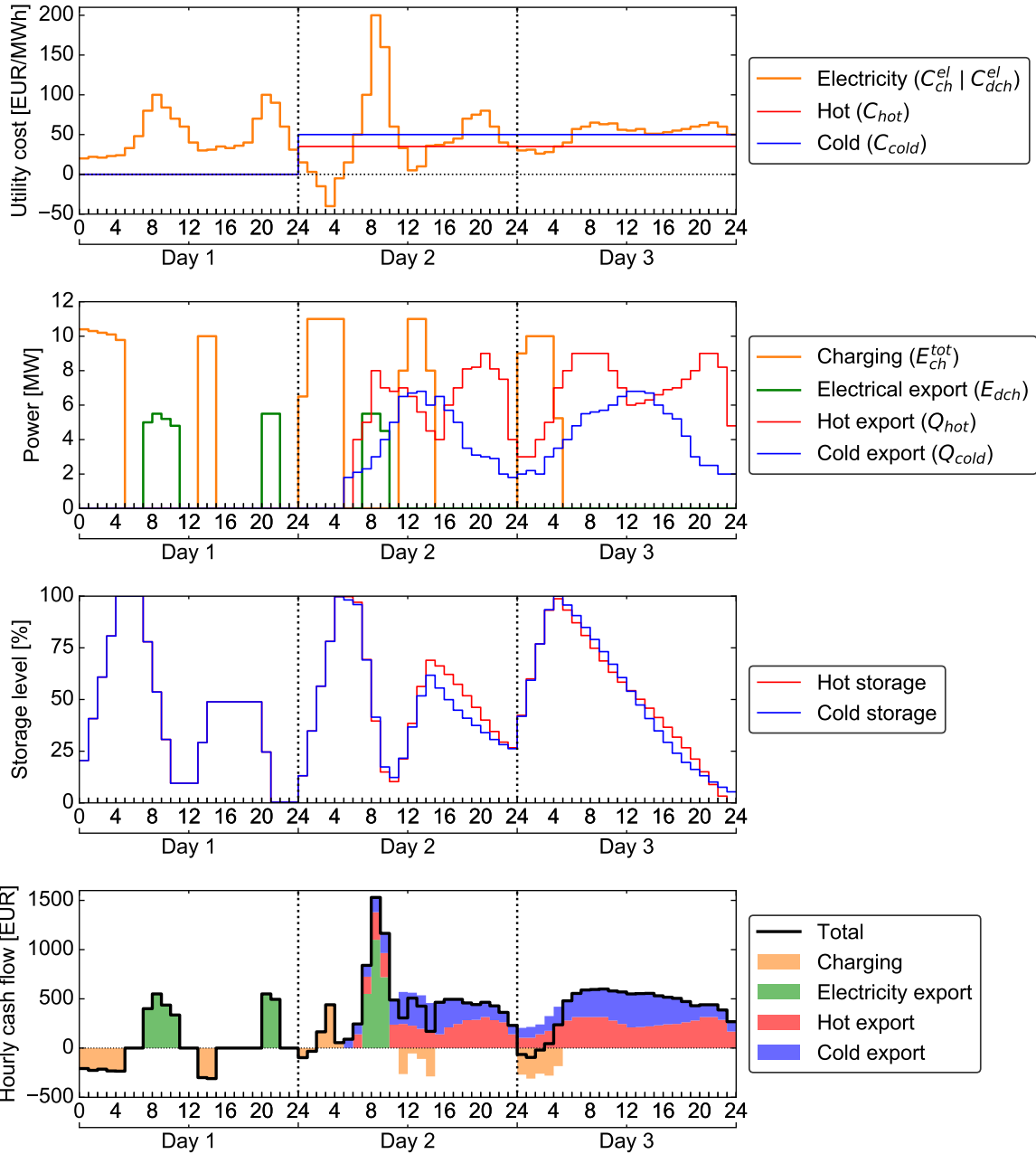


Figure 7: Use case of a 3-TES system for three typical days with varying energy demands and utility prices.

operated as a heat pump with storage system, i.e. without activating the re-electrification ($\gamma^{th} = 100\%$). In this day, the system is fully charged at the beginning of the day when the electricity prices are low and the hot and cold storages allow to adapt to the varying demand of the hot and cold consumers.

The expected cash flows derived from charging and export of each form of energy for the 3-TES system presented in this exemplary use case show a much higher profitability of the system when exporting thermal energy in the form of heat and cold. The summary of the cash flows for each day shown in Table 3 allow to depict the smaller revenue derived from a pure electricity storage system (Day 1) compared to a tri-generation (Day 2) or bi-generation (Day

3) energy system providing heating and cooling only. The absolute figures subject to several assumptions and simplification may be questioned for their exactness, it can be clearly seen on a relative basis that the profitability of the system is increased by a factor 9 to 10 by making use of the tri-generation capability.

Day	Charging	Electrical export	Hot export	Cold export	TOTAL
1	-1726	2768	-	-	1042
2	-188	2370	4071	3885	10138
3	-1303	-	5824	5200	9720

Table 3: Daily cash flows of the 3-TES system presented in Figure 7 (in EUR).

CONCLUSIONS AND INTERPRETATIONS

The novel tri-generation energy storage concept, derived from a pure electrical-to-electrical system is introduced as a large scale energy hub that combines the supply and storage of hot, cold, and electricity in a single system. As shown in Figure 8, other energy storage systems may provide higher achievable electrical-to-electrical round-trip efficiencies, however the moderate temperature levels at which the 3-TES system operates makes it unique and appropriate to combine with plenty of heating and cooling applications. The temperature and pressure levels permit natural process medium (CO₂ and water) and off-the-shelf equipment with high technology readiness level (TRL).

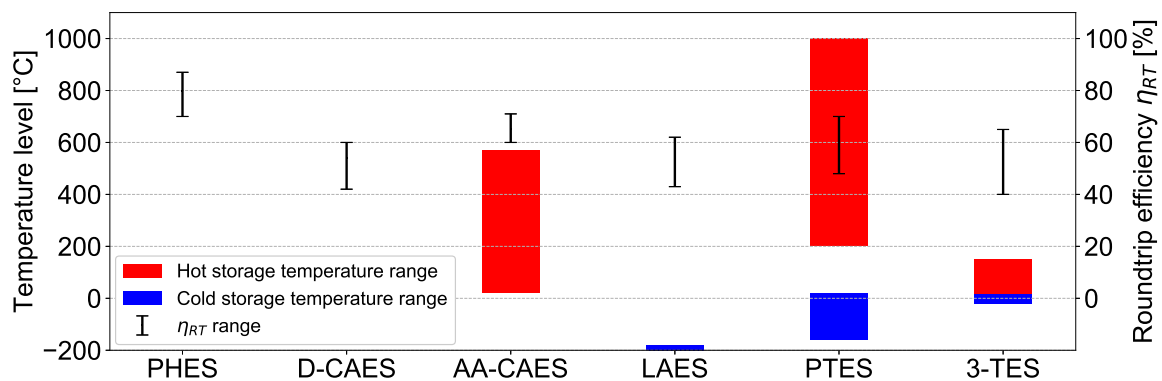


Figure 8: Large-scale energy storage technologies classified by performance and storage temperature ranges [10] [11] [12] [13].

The multiple application boundary conditions influence 3-TES performance and profitability significantly and therefore, the design is dependent on the specific application. Accurate energy demand forecast, and how it varies throughout the plant's lifetime, is important for maximizing system flexibility utilization. Energy prices at the plant location provide the basic input to define the system thermal and electric energy exported amounts. The advantage to adapt to electricity price fluctuations determines that markets with high renewable energy share will favor higher γ^{el} configurations. In contrast, 3-TES plants designed to meet a specific thermal demand (hot, cold or both) will adapt their stored energy amount for re-electrification according to the daily thermal demands. The future expected renewable energy increase will produce frequent electricity surplus periods and the 3-TES can be charged with low-cost (or even negative intermittent cost). Hence, a 3-TES operator can combine completely carbon-neutral electrical

and thermal energy supply for profitable operation.

Any system generating more than one form of energy experiences performance compromises. This is also valid for the 3-TES system, which will compromise the hot thermal export efficiency to obtain the best achievable cold export performance, and vice versa. Similarly, thermal export efficiency reduces for optimized re-electrification capability. The additional re-electrification system investment cost (incl. power turbine, generator, pump) is important if the system must generate profit from electricity price fluctuations like peak shaving for instance. In this case, compromises in Π_{ch} and hot storage tank temperatures are made to find the most suited 3-TES configuration for the given site boundary conditions. On the other hand, thermal export demands requiring high Π_{ch} values (see 5(b)) require fewer compromises when the additional electrical discharge is required. It makes therefore the system more attractive for solutions with high supply temperatures or when hot export is prioritized over cold.

Few consumers require in fact the three forms of energies at the exact matching quantities, therefore, the 3-TES is particularly suitable for **sector coupling** applications, where large renewable energy amounts can be efficiently converted into the three forms of final energy consumed, i.e. hot, cold and electricity. The large design and operational flexibility provided by the 3-TES system (see use case as of Figure 7) allows not only to deliver the requested amount of each form of energy but also increase the return on investment, by profiting on daily fluctuations of the electricity market. This trend is expected to further increase in the upcoming years as renewable energy's share on the electricity generation mix increases.

As presented by the exemplary case study shown in Figure 7 and Table 3, the profitability of the 3-TES system depends strongly on the energy costs at a site, mainly the daily fluctuations of the electricity prices. The operation favoring rather the electrical or thermal export can be decided depending on the daily forecasts and actual demands, knowing the state of charge of the system. Moreover, the time to charge the system can be decided freely, preferably during the low or even negative tariffs periods. This versatility gives the 3-TES system operator insurance to reach his predicted profitability target or even optimize it over time, as the electricity load profiles may change over time. While currently a predominantly thermal export operation might look like a more profitable option, the higher electricity price fluctuations that will be caused by the integration of renewable energy sources in the energy mix should gradually favor the export of electrical energy over thermal.

REFERENCES

- [1] REN21. Renewables 2019 Global Status Report. <https://www.ren21.net/reports/global-status-report/>.
- [2] Mercangöz M., Hemrle J., Kaufmann L., Z'Graggen A., and Ohler C. Electrothermal energy storage with transcritical CO₂ cycles. *Energy*, 45(1):407–415, 2012.
- [3] Morandin M., Maréchal F., Mercangöz M., and Buchter F. Conceptual design of a thermo-electrical energy storage system based on heat integration of thermodynamic cycles - Part a: Methodology and base case. *Energy*, 45:375–85, 2012.
- [4] Morandin M., Maréchal F., Mercangöz M., and Buchter F. Conceptual design of a thermo-electrical energy storage system based on heat integration of thermodynamic cycles - Part b: Alternative system configurations. *Energy*, 45:386–96, 2012.

- [5] Morandin M., Mercangöz M., Hemrle J., Maréchal F., and Favrat D. Thermo-economic design optimization of a thermo-electric energy storage system based on transcritical CO₂ cycles. *Energy*, 58:571–587, 2013.
- [6] Sanz Garcia L., Jacquemoud E., and Jenny P. Thermo-Economic Heat Exchanger Optimization for Electro Thermal Energy Storage based on Transcritical CO₂ Cycles. *3rd European supercritical CO₂ Conference*, September 2019.
- [7] Heat Roadmap Europe. Profile of heating and cooling demand in 2015. https://www.heatroadmap.eu/sp_faq/heat-roadmap-europe-3-stratego-2015/.
- [8] E. W. Lemmon, , Ian H. Bell, M. L. Huber, and M. O. McLinden. NIST Standard Reference Database 23: Reference Fluid Thermodynamic and Transport Properties-REFPROP, Version 10.0, National Institute of Standards and Technology, 2018.
- [9] Jun Lan Zang, Yi Tai Ma, Mi Xia Li, and Hai Qing Guan. Exergy analysis of transcritical carbon dioxide refrigeration cycle with an expander. *Energy*, 30:1162-1175, 2005.
- [10] Andreas V Olympos et al. Progress and prospects of thermo-mechanical energy storage - a critical view. *Progress in Energy* 3, 2021 022001.
- [11] Jacob T. Pumped storage in switzerland — an outlook beyond 2000. *The Economist*, March 2011.
- [12] Adriano Sciacovelli, Yongliang Li, Haisheng Chen, Yuting Wu, Jihong Wang, Seamus Garvey, and Yulong Ding. Dynamic simulation of Adiabatic Compressed Air Energy Storage (A-CAES) plant with integrated thermal storage – Link between components performance and plant performance. *Applied Energy*, 185(P1):16–28, 2017.
- [13] Edward Barbour, Dimitri Mignard, Yulong Ding, and Yongliang Li. Adiabatic compressed air energy storage with packed bed thermal energy storage. *Applied Energy*, 155:804–815, October 2015.